LAWRENCE
LIVERMORE
NATIONAL
LABORATORY

UCRL-CONF-212695

Monte Carlo Particle Transport: Algorithm and Performance Overview

N.A. Gentile, R.J. Procassini, H.A. Scott

June 6, 2005

5 Lab Conference on Computational Hydrodynamics and Transport
Vienna, Austria
June 20, 2005 through June 23, 2005

Monte Carlo Particle Transport: Algorithm and Performance Overview

N. A. Gentile, R. J. Procassini and H. A. Scott

Lawrence Livermore National Laboratory, Livermore, California, 94551

Monte Carlo methods are frequently used for neutron and radiation transport. These methods have several advantages, such as relative ease of programming and dealing with complex meshes. Disadvantages include long run times and statistical noise. Monte Carlo photon transport calculations also often suffer from inaccuracies in matter temperature due to the lack of implicitness. In this paper we discuss the Monte Carlo algorithm as it is applied to neutron and photon transport, detail the differences between neutron and photon Monte Carlo, and give an overview of the ways the numerical method has been modified to deal with issues that arise in photon Monte Carlo simulations.

Neutron Monte Carlo Transport

The Monte Carlo method of simulating particle transport is a *statistical* approach to "solving" the linearized Boltzmann equation, which is shown below for neutrons:

$$\begin{aligned}
&\frac{1}{v}\frac{\partial \psi(\vec{r},E,\Omega,t)}{\partial t} + && \text{(Temporal Streaming)}\\
&(\nabla\cdot\Omega)\psi(\vec{r},E,\Omega,t) + && \text{(Spatial Streaming)}\\
&\Sigma_a(\vec{r},E)\psi(\vec{r},E,\Omega,t) = && \text{(Collisional Absorption)}\\
&\int_{E'}\int_{\Omega'}\Sigma_s(\vec{r},E',\Omega' \rightarrow E,\Omega)\psi(\vec{r},E,\Omega,t)\,d\Omega'\,dE' + && \text{(Collisional Scattering)}\\
&\chi(E)\int_{E'}\nu(E')\Sigma_f(\vec{r},E')\int_{\Omega'}\psi(\vec{r},E,\Omega,t)\,d\Omega'\,dE' + && \text{(Collisional Fission Source)}\\
&S_{ext}(\vec{r},E,\Omega,t) && \text{(External Source)}
\end{aligned} \qquad (1)$$

where $\psi(\vec{r},E,\Omega,t)$ is the angular flux, $\Sigma_a(\vec{r},E)$ is the macroscopic cross section for particle absorption, $\Sigma_s(\vec{r},E',\Omega' \rightarrow E,\Omega)$ is the macroscopic cross section for particle scattering, $\Sigma_f(\vec{r},E')$ is the macroscopic cross section for particle production from fission, $\chi(E)$ is the secondary particle spectrum emitted from the fission process, $\nu(E')$ is

the average number of particles emitted per fission, $S_{ext}(\vec{r}, E, \Omega, t)$ is an external source, $\vec{r}$ is the spatial coordinates, E is the energy, Ω is the angular direction and t is time.

While the spatial domain is divided into cells or regions, and energy may be divided into groups, this method does *not* employ a *continuum* approach to solve this integro-differential equation (Equation 1), as is the case in deterministic transport methods, such as the S_N or P_N methods. In many transport applications, each Monte Carlo simulation particle represents an *ensemble* of physical particles. The essence of the Monte Carlo method of particle transport is to follow, or track, the trajectory of individual particles through this seven-dimensional phase space in an analog fashion. The trajectory, or track, of each particle through phase space is comprised of several segments, each of which is terminated by a discrete event.

In this approach, particles undergo a series of events during tracking. The first of these is particle streaming to the end of the time step, known as a c*ensus event*, which represents the Temporal Streaming term (see Equation 1). The next event is streaming to the boundary of a neighboring cell, region or system boundary, known as a *facet crossing event*, representing the Spatial Streaming term. A special subcase is streaming to the system boundary resulting in leakage from the system, known as an *escape event*. The interaction of a particle with an atom or nucleus in the background medium is known as a *collision event*, representing the Collisional Absorption or Collisional Scattering terms. A special subcase of collision absorption are collisional interactions that result in the production of secondary particles, which is represented by the Collisional Fission Source term. Two additional events are possible during the transport of charged particles. These particles are assumed to undergo continuous slowing down and deflection due to small-angle Coulomb scattering off the of the electrons in the background medium. These additional events are streaming to the lower-energy group boundary or to the thermal energy of the medium, known as an *energy-boundary crossing* or *thermalization* event, respectively. Note that the proceeding discussion, while focused on neutron transport, is broadly applicable to transport of all types of particles, although additional or alternate physical interaction mechanisms may be involved.

This event-based particle tracking scheme is illustrated in Figure 1 for neutral particles being transported through a mesh-based problem geometry. This figure shows a two-dimensional mesh of 6 x 4 = 24 zones with three materials distributed throughout the mesh. Three individual track segments are shown, along with the distances to each of the terminating events. Note that the segment tracks are actually colinear, but have been separated for illustrative purposes. The Monte Carlo method of particle transport selects the *shortest* event distance as the terminating event of the segment. For the segment in the lower left corner of the figure that starts in Material A, the distances to census (shown in blue) and collision (shown in green) would take the particle outside of the extent of the current zone. As a result, the shortest distance to cross a facet into a neighboring zone, based upon the direction of particle travel (shown in red), is the terminating event for that segment. For the segment in the center of the figure that starts in Material B, the distance to collision is shorter than either the distance to facet crossing or census, hence the particle will undergo a collision in the current zone, but as shown in the figure, not necessarily

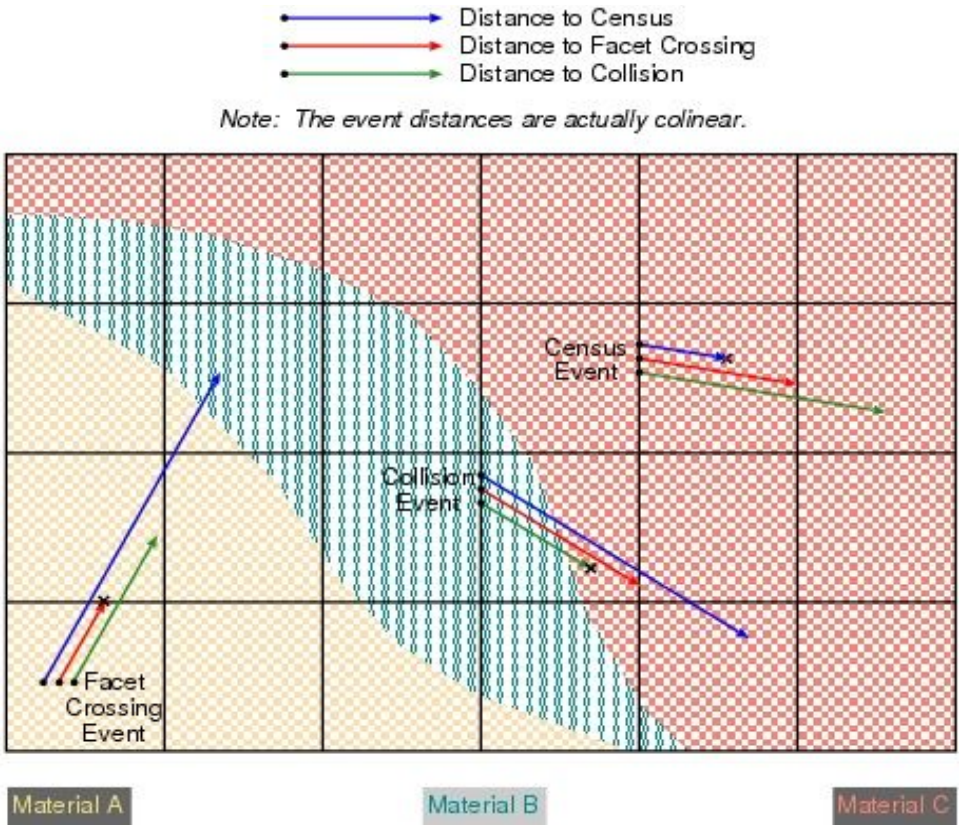

Figure 1. Track segments from three individual neutral particle trajectories through a two-dimensional mesh that contains three materials. For each segment, the distances to census (blue), facet crossing (red) and collision (green) are shown separated for illustrative purposes. The method selects the shortest of the three event distance for each segment.

in the material that the segment began in. For the upper-right segment in the figure, which starts in Material C, the distance to the end of the time step (census) is the shortest, such that the particle will be placed back into the particle "vault" for tracking in the next cycle. Particles are typically tracked in a three-dimensional Cartesian space which is independent of the problem geometry or mesh. In this case, a neutral particle travels in a straight line until it intersects a facet/surface of first order (plane), second order (sphere, cylinder, cone, ellipsoid), etc, which forms the boundary of a zone or regions, or the exterior of the system.

Some additional features of the Monte Carlo particle transport method are as follows. While the particles may have discrete but continuously-varying energies, the multigroup treatment of energy employs cross sections which are assumed to be constant within a group. Collisions are treated as point events, such that only the direction of the particle is changed, and not its spatial location. Collisions may result in the production of secondary particles via transmutation reactions. If this occurs, then those secondary particles which are being tracked (say, neutrons and gammas) are placed in the particle "vault" for subsequent tracking, while those secondary particles which are not being tracked (say,

protons) are assumed to be locally deposited, in terms of both mass and energy.

The approximation of the flux in a given zone (z) and energy group (g) is sum of the particle (j) path lengths (L) through the volume (V_z) in a given time step (Δt):

$$\phi_{z,g} = \sum_j \left(\frac{W_j \; L_{j,g}}{V_z \; \Delta t} \right) \tag{2}$$

These fluxes are multiplied by the number densities (n_i) of background isotopes (i) and the relevant cross sections $(\sigma_{r,i})$ to produce rates of energy deposition and isotopic production/depletion:

$$R_{r,z,g} = \sum_i \phi_{z,g} n_{i,z} \sigma_{r,i,g} \tag{3}$$

Each Monte Carlo simulation particle is defined by a set of attributes, which can include spatial coordinates: $(x,\ y,\ z)$, velocities or direction cosines $(v_x,\ v_y,\ v_z)$ or $(\cos(\alpha),\ \cos(\beta),\ \cos(\gamma))$, kinetic energy E, weight (defined as the the ratio of the number of physical particles represented by each simulation particle) $W = \left(N_{phys} / N_{sim} \right)$, the time to census t_{cens}, the number of mean-free paths remaining before a collision must be enforced N_{mfp}, the random number seed R_{seed} (for applications using per-particle seeds), and a number of miscellaneous attributes including the number of collisions that the particle has undergone, last event the particle experienced, the breed particle (describing the material it was created in, the process by which it was created, etc.), the spatial domain, cell, facet, etc. These particles are usually tracked in the seven-dimensional phase space comprised of three spatial coordinates $(x,\ y,\ z)$, three velocities $(v_x,\ v_y,\ v_z)$ or two-directions (Ω) and energy (E), and time (t).

Monte Carlo Algorithms for Calculating Criticality Eigenvalues

Two eigenvalue forms of the Boltzmann transport equation are typically used to define the criticality of a system. The first is the (ν / k_{eff}) form which describes a balance between neutron production and removal in a static, source-free multiplying medium:

$$\begin{aligned} (\nabla \cdot \Omega)\psi(\vec{r}, E, \Omega, t) \; + \Sigma_a \psi(\vec{r}, E, \Omega, t) \; = \\ \int_{E'} \int_{\Omega'} \Sigma_s(\vec{r}, E', \Omega' \; \rightarrow \; E, \Omega) \psi(\vec{r}, E, \Omega, t) d\Omega' dE' \; + \\ (\chi(E) / k_{eff}) \int_{E'} \nu(E') \Sigma_f(\vec{r}, E') \int_{\Omega'} \psi(\vec{r}, E, \Omega, t) d\Omega' dE' \end{aligned} \tag{4}$$

where k_{eff} is the balance parameter which is used to determine if the system is subcritical $(k_{eff} < 1)$, critical $(k_{eff} = 1)$ or supercritical $(k_{eff} > 1)$. The second is the (α / ν) "static" form, which is derived from the following separability of variables ansatz:

$$\psi(\vec{r}, E, \Omega, t) = \varphi(\vec{r}, E, \Omega)\, \zeta(t) \tag{5}$$

and the assumption that the system has "evolved" to its fundamental eigenmode (the eigenmode with the largest eigenvalue, such that all other eigenmodes with smaller eigenvalues have been diminished to zero):

$$\zeta(t) = \zeta(0) e^{\alpha t} \tag{6}$$

to give:

$$\begin{gathered}(\nabla\cdot\Omega)\psi(\vec{r}, E, \Omega, t) + (\Sigma_a + (\alpha/v))\psi(\vec{r}, E, \Omega, t) = \\ \int_{E'}\int_{\Omega'} \Sigma_s(\vec{r}, E', \Omega' \rightarrow E, \Omega)\psi(\vec{r}, E, \Omega, t)\, d\Omega' dE' + \\ \chi(E)\int_{E'} \nu(E')\Sigma_f(\vec{r}, E')\int_{\Omega'} \psi(\vec{r}, E, \Omega, t)\, d\Omega' dE'\end{gathered} \tag{7}$$

where α is the parameter that describes the logarithmic growth rate of particles in the system. For a subcritical system $(\alpha < 0)$, the (α/v) terms leads to "time production" of particles, while for a supercritical system, the (α/v) terms leads to "time absorption" of particles (the term "time" is used because the used of α are inverse time).

Some *static* algorithms for calculating the k_{eff} or α eigenvalues of a system include:

(1) The *Static k* method, which "solves" the (ν/k_{eff}) form of the Boltzmann equation by iterating to convergence over many generations.

(2) The *Static* α method, which "solves" the (α/v) form of the Boltzmann equation by adding "time absorption" ("time production") of neutrons in supercritical (subcritical) systems and iterating to convergence.

(3) The *Pseudo-dynamic* α method, which "solves" the Boltzmann equation for a fixed background medium, evolving the neutron distribution to convergence *in time* over many *settle cycles*.

These static k_{eff} and α eigenvalues are calculated from iteration or cycle averaged values of the neutron production (P), absorption (A), leakage (L) and removal lifetime (τ_{rem}) via:

$$k_{eff} = \frac{\langle P \rangle}{\langle A \rangle + \langle L \rangle} \tag{8}$$

and

$$\alpha = \left(\frac{1}{\langle \tau_{rem} \rangle}\right)\left(\frac{\langle P \rangle}{\langle A \rangle + \langle L \rangle} - 1\right) = \left(\frac{1}{\langle \tau_{rem} \rangle}\right)\left(k_{eff} - 1\right) \tag{9}$$

Averaged quantities are employed in the calculation of the *static* k_{eff} or α eigenvalues

in order to reduce the stochastic noise by averaging over many settle iterations/cycles.

A *dynamic* algorithm that is used to calculate the α eigenvalue of a system is:

The *Dynamic* α method uses the separability of variables ansatz (Equation 5) and fundamental eigenmode assumption (Equation 6) to give α at cycle n:

$$\alpha^n = \left(\frac{1}{\Delta t^n}\right) \ln\left(\frac{N(t^n)}{N(t^{n-1})}\right) \qquad (10)$$

where $N(t^n)$ is the particle population at the end of cycle n.

The logarithm of the population ratio used in the calculation of the *dynamic* α eigenvalue can lead to increased stochastic noise. This occurs as $\Delta t \to 0$, which results in $N(t^n) \to N(t^{n-1})$, and hence $\ln(N(t^n)/N(t^{n-1})) \to 0$.

Accuracy Considerations of Monte Carlo Calculations

Since the Monte Carlo method does not solve the Boltzmann equation via use of numerical differences and quadratures, it does not incur many of the accuracy and stability limitations which are faced by deterministic methods such as S_N or P_N. However, there are several issues which need to be considered when modeling particle-transport with the Monte Carlo method.

Given *enough particles* the Monte Carlo method is capable of sampling all of the seven-dimensional phase space $(x, y, z, \cos(\alpha), \cos(\beta), \cos(\gamma), E, t)$ spanned by the Boltzmann equation. However, since it is a statistical method, there is no such practical concept as "enough particles". The calculated results should *always* be accompanied by an estimate of the error which is based upon the number of particles used in the calculation. In addition, accurate modeling of collision interaction and flux attenuation requires zone spacings comparable to, or smaller than, a mean-free path length $\Delta x \le \lambda_{mfp}$. Furthermore, the multigroup energy treatment limits the resolution of rapidly-varying cross section structures, such as resonances, lines or edges, which leads to inaccuracies in the calculation of resonant self-shielding. Lastly, one should be aware that approximations may be used , such as equally-probable bins, when sampling the energy and angle of secondary particles emerging from collision events.

With regard to the particle counts required for reasonably accurate simulations, the following guidelines can be used. The number of simulation particles (N_{sim}) required for static k_{eff} or α eigenvalue calculations can be as low as 10^3 to 10^5 ,since the production, removal and lifetime components used to calculate the eigenvalues are averaged over many settle iterations/cycles, and because static eigenvalues are *global* quantities which *do not* require large per-zone particle counts. In contrast, the number of simulation particles (N_{sim}) required for time-dependent depletion calculations (such as a reactor depletion calculation) *must be significantly larger*, of order 10^5 to 10^9, since energy deposits and isotopic depletion/production require a sufficient number of particles per zone, of order 10 to 1000, in order to reduce statistical fluctuations in those quantities.

Implicit Monte Carlo

Photon Monte Carlo differs from neutron Monte Carlo in two ways. First, photons always move with speed c, instead of with a spectrum of velocities as neutrons do. This is a minor difference that makes tracking the particles in Monte Carlo photon simulations slightly easier. The second difference is much more important. This difference is that the absorption and emission – the coupling – of photons to the matter temperature has to be simulated also. This coupling can be very non-linear and can make the solution of photon Monte Carlo difficult when matter and radiation are near equilibrium. When this occurs, absorption and emission are both very large and nearly equal. The changes in the radiation field and matter energy are functions of the small difference between large quantities. This causes the method to exhibit large fluctuations and require very small time steps (Fleck, 1963).

These symptoms result from a lack of implicitness in the photon Monte Carlo solution technique. The absorption of energy from a photon by matter is equal to $e^{-\sigma d}$, where d is the distance traveled by the photon. This quantity is calculated for each particle in the simulation at many times during each time step. In effect, it is centered in the middle of the time step.

The emission from the matter is proportional to $\sigma c a T^4 V \Delta t$. Here σ is the Planck mean opacity, c is the speed of light, T is the matter temperature, V is the volume, and Δt is the time interval under consideration. The dependence of the emission on the fourth power of the temperature makes the emission highly nonlinear in T. The matter temperature is known only at the beginning of the time step. Thus the emission term is centered at the beginning of the time step.

The difference between the centering of these two nearly equal terms is the cause of the problems photon Monte Carlo has near equilibrium. The different centering means that the emission that is calculated for a time step does not reflect the heating of the zone by radiation during the time step. If an initially cold, opaque zone is exposed to a large incoming flux of radiation, the zone will absorb a great deal of energy, but it does not radiate accordingly. The temperature will increase by too large an amount. On the next time step, the zone, which is too hot, will radiate too much energy, since T is too large. This leads to large fluctuations in the matter temperature unless very small time steps are taken. The value of Δt must be small enough that the matter temperature anywhere in the problem does not change very much during any time step.

In order to remove this restriction on the time step, Fleck and Cummings developed the Implicit Monte Carlo method (Fleck and Cummings, 1971). This technique uses an estimate of the future matter temperature derived from the matter energy equation in the emission term of the radiation transport equation. It should be emphasized that this is not an extrapolation of the matter temperature. It is an expression for the future temperature as a function of the current temperature, the opacity, the equation of state of the material, and the size of the time step. This expression is inserted into the transport equation. When the terms in this new equation are grouped together, the effect is that the amount of

absorption and emission is reduced, and a new term that simulates isotropic scattering is added.

The effect is that some fraction of the absorption opacity is replaced by a scattering opacity. This change has a physical interpretation. In thermal equilibrium, photons are absorbed and then quickly re-emitted. In photon Monte Carlo simulations, the absorption is simulated accurately, but the re-emission is not, because the initial matter temperature was used to calculate the emission. Implicit Monte Carlo simulates the absorption and subsequent re-emission by a scatter. This scattering is called effective scattering, to differentiate it from physical scattering that may also be occurring in the simulation. Adding this effective scatter to the Monte Carlo simulations almost always allows much larger time steps to be taken. However, the replacement of absorption with effective scattering can lead to large simulation times, as photons undergo many computationally expensive scatters instead of being quickly absorbed.

In the next section, we will examine the equations of Monte Carlo photon transport and show how the algorithm of Fleck and Cummings is developed. In the next section we will give an example problem that demonstrates that it removes the time step restriction.

The Equations of Implicit Monte Carlo

Radiation transport problems require the solution of two coupled equations:

$$\frac{1}{c}\frac{\partial I}{\partial t} + \Omega \bullet \nabla I = -(\sigma_s + \sigma_a) I + \frac{1}{4\pi} c \sigma_a a T^4 b(\nu, T) + \int \sigma_s I \, d\nu \, d\Omega + S_I \quad (1)$$

$$\frac{\partial \varepsilon}{\partial t} = \int \sigma_a I \, d\nu \, d\Omega - c a T^4 + S_\varepsilon \quad (2)$$

Here $I(x,\Omega,t,\nu)$ is the radiation specific intensity, with cgs units erg/(cm^2 Hz steradian s); $\varepsilon(x,t)$ is the matter energy density, with cgs units erg/cm^3; $\sigma_a(x,t,\nu)$ is the absorption opacity, with cgs units cm^{-1}; σ_s is the scattering opacity; σ_P is the Planck mean opacity; $b(\nu,T)$ is the normalized Planck function; S_I represents photon sources, for example lasers; and S_ε represents thermal sources, for example, chemical reactions. Coupling between I and ε is through T^4 and σ_a terms. The aT^4 term in the transport equation is a source from the matter into the radiation field, and describes thermal emission. The aT^4 term in the matter energy equation is the corresponding sink, describing energy lost by the matter.

Implementing the Implicit Monte Carlo algorithm has 3 steps:

- The matter energy equation is manipulated to get an expression for the time derivative of T^4
- This derivative is approximated to get an expression for T^4 at the end of the time step in terms of current T, absorption, etc.
- This expression for T^4 is substituted into the transport equation and the matter energy equation

The result of this procedure is a pair of altered equations for I and ρ, not the same equations with a different value for T in the emission term. These new equations for I and ρ are usually more stable than the original set.

This procedure is described in detail in (Fleck and Cummings 1971). A brief description will be provided here. First, we define the radiation energy density $\rho = a T^4$. Then we define the quantity $\beta = d\rho/d\rho$ which, by the chain rule, is equal to $4aT^3/(\rho c_V)$. Here, c_V is the heat capacity. Defining these quantities allows us use Eq. 2 for the time derivative of e to get a time derivative of ρ:

$$\frac{\partial \rho}{\partial t} = \beta \frac{\partial \rho}{\partial t} = \beta \left[\sigma_a I \, d\Omega \, d\nu - \rho c \sigma_P \right] + \beta S_\rho \quad (3)$$

The second step is to use this value of the time derivative to estimate the value of ρ at the end of the time step. We do this by forward differencing the time derivative on the left side of the equation, using the (unknown) end of time step value for ρ on the right side, and using the values for the other quantities β, T etc at the beginning of the time step. This gives us an equation we can solve for the end of time step radiation energy density. The result is

$$\rho^{n+1} = \frac{1}{1 + \beta c \sigma_P \Delta t} \rho^n + \frac{\beta c \Delta t}{1 + \beta c \sigma_P \Delta t} \left[\sigma_a I \, d\Omega \, d\nu + \frac{1}{1 + \beta c \sigma_P \Delta t} \beta \Delta t S_\rho \right] \quad (4)$$

Here, the superscript n denotes values at the end of time step n, and $n+1$ denotes end of time step values. The third step in the Fleck and Cummings algorithm is to use this estimate for ρ^{n+1} in the thermal source term ($\sigma_P c \, aT^4$) in the transport equation Eq. 1 and the energy sink term of the matter energy equation Eq. 2. The results are

$$\begin{aligned} &\frac{1}{c}\frac{\partial I}{\partial t} + \Omega \bullet \nabla I = -(\sigma_s + \sigma_a) I + \frac{1}{4\pi} f c \sigma_a b_\nu a T^4 b(\nu, T)\Big|^n \\ &+ \frac{1}{4\pi}(1-f)\sigma_a b(\nu, T) \int \sigma_a I \, d\Omega \, d\nu + \\ &+ \int \sigma_s I \, d\Omega \, d\nu + \frac{1}{4\pi}(1-f)\frac{\sigma_a b(\nu, T)}{\sigma_P} S_\rho + S_I \quad (5) \end{aligned}$$

and

$$\frac{\partial \rho}{\partial t} = \int f \sigma_a I \, d\Omega \, d\nu - f c \sigma_a b_\nu a T^4 b(\nu, T)\Big|^n + f S_\rho \quad (6)$$

The quantity $f = 1/(\beta c \sigma_P \Delta t)$ arises several times in this equation. This quantity is often referred to as the "Fleck factor". It takes on values between 0 and 1.

Equations 5 and 6 are the new equations that the IMC method solves. There are several differences from the original equations Eq.1 and Eq.2. The thermal emission in both equations has been reduced by the factor f, because f now multiplies σ_a. Scattering has been added with opacity $(1-f)\sigma_a$. This scattering is isotropic in direction and has a frequency distribution given by the Planck function. Thus it resembles thermal emission it replaces. A fraction $(1-f)$ of the matter energy source S_ρ has been removed from the matter source and added to the photon source. This new term in the modified transport

equation represents thermal emission from the matter heated by the matter source during the time step.

When f approaches 1, the pair Eqs. 5 and 6 approaches the original set of Eqs. 1 and 2. This occurs under several circumstances:

- The time step Δt is small. In this case, the temperature changes very little between time n and time $n+1$.
- σ_P is small. If the material has a small Planck mean opacity, then the coupling between the matter and radiation is small, and the matter temperature is not changing rapidly.
- c_V is large, making β small. When the heat capacity is large, the matter temperature does not change much even if the material absorbs a large amount of energy.

In the other limit, f is small, approaching zero. This happens when σ_P or Δt is large, or c_V is small. Physically, this situation occurs when the matter and radiation are strongly coupled. The matter temperature and radiation temperature should be very nearly equal, and any increase in the matter temperature would result in the emission of photons to maintain $T_m \approx T_r$. Particles in the simulation scatter many times while depositing very little energy, and the emission term in Eqs. 5 ands 6 is small because $f \sigma_a$ is near zero. In the original Monte Carlo algorithm (henceforth MC), strong coupling lead to oscillations unless the time step was very small. In IMC simulations, the time step can remain relatively large, but the computational expense of simulating the many scatters can be prohibitive.

In the next section, we will show that the IMC algorithm, which solves these new equations allows us the run a test problem stably with a much larger time step than the MC algorithm described in (Fleck 1963). This original algorithm is equivalent to running IMC with f set to 1.0. We will also show problems for which the change of absorption into scattering causes an IMC simulation to take a prohibitive amount of computer time.

Results of Implicit Monte Carlo

The first test problem we will examine is a simple one-dimensional test. A material with an initial temperature of 0.01 keV is heated at x = 0 with a temperature source of 1.0 keV. The material has an ideal gas equation of state with $c_V = 1.0 \times 10^{14}$ erg cm^{-3} keV^{-1}. The absorption opacity is 100 cm^{-1}. The density is fixed at 1.0 gm cm^{-3}. The simulation takes place on a mesh of 200 zones each with $\Delta x = 0.01$ cm.

The diagnostic in the test is the temperature of the first zone. In nature, this temperature would rise smoothly from the initial value of 0.01 keV to the source temperature 1.0 keV without overshooting. In a simulation, we would like to reproduce this behavior. For small values of Δt we will, but for larger values we will see overshoots.

In Fig. 1 we compare the behavior of MC and IMC by plotting the temperature in the first zone for the first ten time steps in the simulation. When a Δt of 1.0×10^{-4} ns is used, MC and IMC produce the same answer. When Δt is raised to 2.5×10^{-4} ns, MC shows a

slightly faster rise in the temperature. When Δt is raised to 5.0 x10^{-4} ns, the Monte Carlo solution begins to oscillate, and, on the eighth cycle, yields a temperature that is less than zero, at which point the simulation fails. With this value for Δt, the IMC simulation is still stable. With a Δt of 1.0 x10^{-1} ns, IMC shows a slight overshoot in the temperature, but it rapidly relaxes to the final, correct value of 1.0 keV. On this test problem, IMC is capable of running with a time step 500 times greater than the one that causes the MC simulation to fail.

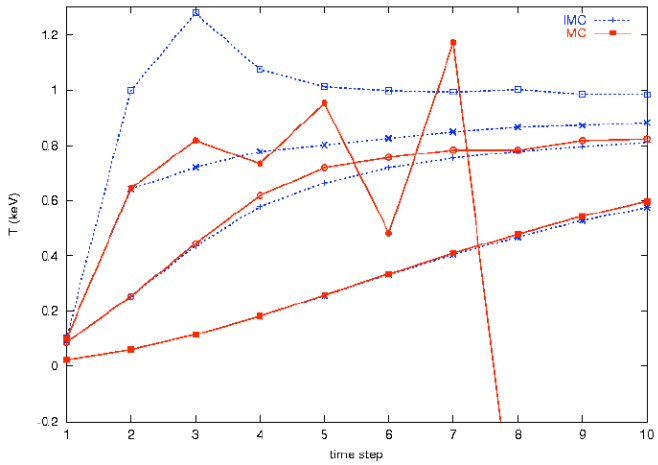

Figure 1. Plot of Temperature vs. time step number for various values of Δt for both IMC and MC. Values of Δt in ascending order for pairs of curves on the plot are 1.0x10^{-4} ns, 2.5 x10^{-4} ns, 5.0 x10^{-4} ns, and 1.0 x10^{-1} ns.

The second test problem is a two-dimensional test known as the crooked pipe. This test takes place on an RZ mesh. An initially cold region with small opacity is heated with a time-independent temperature source. A region with large opacity impedes the radiation flow, which travels along a crooked path around the large opacity region while heating it. The diagnostic quantities are the temperatures at five points in the small opacity region. This test was developed by (Graziani and LeBlanc 2000). Details on the mesh and IMC simulations are given in (Gentile 2001).

This problem has a large amount of material with a large opacity that becomes hot. This causes f to become very small – on the order of .001 – in a significant part of the problem. As the opaque material becomes hot, many effective scatters take place, and the simulation time becomes large.

Fig. 2 shows the temperature vs. time for two IMC simulations. One ran on a two-dimensional RZ mesh and the other on a three-dimensional mesh that was one zone thick in the angular direction (that is, a wedge). It also shows the results of an S_N simulation (Nowak and Nemanic 1999).

All three codes show good agreement. However, the run time for the IMC simulations was prohibitive. The three-dimensional run took over 159 hours on one 533 MHz. DEC

alpha processor. This test problem demonstrates that IMC, while accurate, can have very large run times on problems with *f* near zero in large regions.

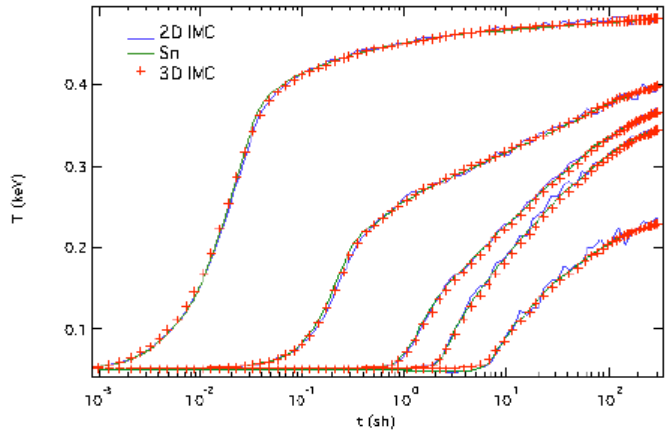

Figure 2. Plot of Temperature vs. time step number for five points in the crooked pipe test problem. IMC and S_N both produce very similar results, but IMC computational expense is large. Time axis units are 10^{-8} s = 10 ns.

Research Directions For Monte Carlo Radiation Transport

Hybrid Methods

IMC run times in opaque systems can be improved by using the diffusion equation. If there are many effective scatters in a zone, the photons execute long sequences of random walks. This results in the particles losing all angular information, for example, their initial direction. When the scattering mean free path, either real or effective, is small compared to the length scale on which the problem quantities vary, the diffusion equation is a good approximation to the transport equation (Larsen 1980). This suggests that we can use solutions to the diffusion equation to accelerate IMC in those regions where it is most computationally expensive.

One method, referred to as the "random walk" procedure, was developed by (Fleck and Canfield 1984). In this procedure, a solution of the diffusion equation in a sphere is used to advance selected particles inside a zone. A sphere is centered on a particle, with the radius chosen such that the sphere is entirely contained in the zone. This is to ensure that there are no discontinuities in material properties inside the sphere. The solution of diffusion equation inside the sphere is expressible as an infinite series, the value of which can be tabulated. This solution is interpreted as a probability distribution for the location of the particle. Sampling from this probability distribution allows the particle to jump in one step to a new location, rather than undergoing many effective scatters.

Fleck and Canfield showed that this procedure could decrease the computational expense of an IMC simulation with opaque material by a factor of approximately 5. A drawback to the method is that the calculation of the sphere for each particle is expensive. Advancing a particle one random walk jump is thus much more expensive than performing one IMC effective scatter, especially on complicated meshes. So the problem

must be such that many effective scatters would take place in each zone for the "random walk" algorithm to make the problem run faster.

Another way to use solutions to the diffusion equation is to invoke what are called hybrid techniques. Hybrid techniques solve the diffusion equation by traditional linear systems methods in opaque regions of the problem, and IMC in others (see Gentile 2000 for a summary.) In hybrid techniques, diffusion is used in opaque regions where IMC is slow, and IMC is used in non-opaque regions where diffusion is inaccurate.

Hybrid techniques require that each method provide boundary conditions for the other method where the opaque and non-opaque regions meet. IMC particles entering the diffusion region are converted into an approximate boundary flux to provide a Marshak-type boundary condition for diffusion. The solution of the diffusion equation yields a flux, which is interpreted as a source of particles into IMC region.

Fig. 3 shows the results for a hybrid IMC/diffusion calculation for the crooked pipe test problem compared to IMC and diffusion results. This is the same quantity (matter temperature) at the same points plotted in Fig. 2. The hybrid method produces results which are very similar to the pure IMC and S_N results. As mentioned above, the pure IMC simulation took 5.73×10^5 s (about159 hours). The hybrid run took 2.42×10^4 s. This is a decrease in computational cost by a factor of greater than 23 (Gentile 2001).

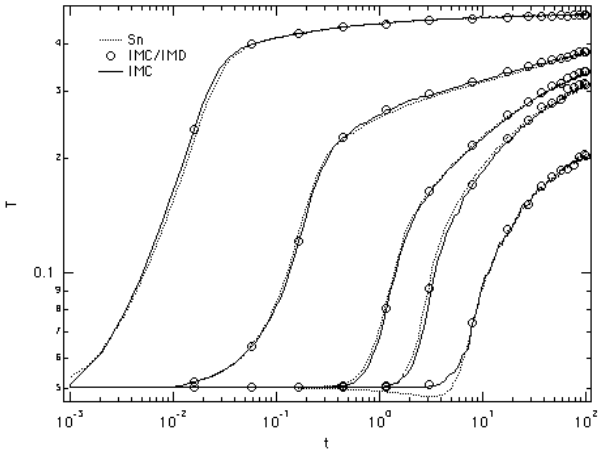

Figure 3. Plot of Temperature vs. time step number for five points in the crooked pipe test problem. IMC, the IMC/IMD hybrid method, and S_N all produce very similar results. Time axis units are 10^{-8} s = 10 ns.

Hybrid methods can yield large decreases in run times on some problems. However, they have several drawbacks. The transport equation gives an outgoing flux and requires an incoming flux as a boundary condition, while the diffusion equation requires a total flux as a boundary condition. Thus the coupling between IMC and diffusion is approximate. Discontinuities in the solution at the boundaries, as well as instabilities, can occur. In addition, hybrid methods are very difficult to implement, especially on complicated meshes.

Symbolic Implicit Monte Carlo

The IMC method of Fleck and Cummings improves the stability of the Monte Carlo method for radiation transport considerably. However, since β remains fixed, the resulting set of equations is a linearized approximation to the full nonlinear equations, akin to the linearized equations commonly used with deterministic methods. In the absence of some convergence procedure, timesteps large enough for the temperature to change significantly will produce linearization errors and, potentially, instability.

An asymptotic analysis by Densmore and Larsen (2004) demonstrates that the Fleck-Cummings method becomes inaccurate for large timesteps, and does not correctly yield the diffusion limit for very small photon mean free paths. A modification of the method due to Carter and Forest (1973) produces the diffusion limit, but only for small timesteps, as it shares the linearized character and concomitant errors of the Fleck-Cummings method.

A method for achieving an implicit non-linear solution, called Symbolic Implicit Monte Carlo (SIMC), was first proposed by Brooks (1989) in the context of line radiation transport. N'kaoua (1991) applied this method to thermal photon transport. In this technique, the weights of the particles are treated as unknowns and are carried symbolically through the tracking procedure. Photons emitted in a zone during a timestep are given weights proportional to T^4. After transporting the photons, the material energy equation becomes a non-linear set of equations for the updated temperatures. This set of equations produces a fully implicit solution for the temperatures, remains stable for very large timesteps and properly captures the diffusion limit. However, the equations couple the temperatures in all zones, with the effective bandwidth determined by the timestep and mean free paths. The need to invert a (potentially-) full matrix presents a difficulty in scaling to very large (or finely zoned) systems.

Difference Formulation

The main impediment to efficiently obtaining accurate solutions with either IMC or SIMC is the slow decrease of statistical noise with the number of photons, or alternatively, the computational expense of tracking through opaque regions where photons undergo very many scatters. Random walk approaches and hybrid methods attempt to address this problem by increasing the efficiency of the transport method by utilizing the diffusion-like behavior of photons in opaque regions. A recent alternative approach, the difference formulation, transforms the equations so that Monte Carlo transport naturally becomes more efficient in opaque regions (Szoke and Brooks, 2005).

The difference formulation casts the radiation transport equations in terms of the difference D between the intensity and its equilibrium value,

$$D(\mathbf{x},t;\nu,\mathbf{\Omega}) \equiv I(\mathbf{x},t;\nu,\mathbf{\Omega}) - B(\nu,T(\mathbf{x},t))$$

The transport equations for the difference intensity,

$$\frac{1}{c}\frac{\partial D}{\partial t} + \Omega \bullet \nabla D = -\sigma_a D - \frac{1}{c}\frac{\partial B}{\partial t} + \Omega \bullet \nabla B \qquad \frac{\partial \varepsilon}{\partial t} = \int \sigma_a D \, d\nu \, d\Omega + S_\varepsilon$$

are completely equivalent to the original equations and obey equivalent boundary and initial conditions. Scattering poses no difficulties, but the discussion here omits

scattering for simplicity.

Since the transformed equation is equivalent to the original, there is no obvious advantage to either formulation for deterministic solution methods (although the differing characters of the source terms may lead to distinct numerical behaviors in certain situations). However, in an opaque region, both the difference intensity and the gradient of the Planckian become small. In particular, the stiff balance between emission and absorption is replaced by small terms. Therefore, one might expect a Monte Carlo transport treatment to benefit greatly from the difference formulation in these regions.

Results to date, which much still be classified as preliminary, have borne out this expectation. Brooks, *et al* (2005) have implemented the difference formulation with SIMC for thermal photon transport. They consider a test problem consisting of a uniform slab with a frequency-independent opacity and constant specific heat that is illuminated from the left side with a 1 keV blackbody radiation field. Figure 4 shows the steady-state solutions for the material temperature for four different optical thicknesses, 1, 10, 100 and 1000 mean free paths. The standard deviations in the results, calculated both with the standard formulation and the difference formulation are also shown. The standard deviations are multiplied by appropriate factors to make them easily visible on the figures.

The two formulations produce the same results (within statistical noise), but the standard deviations in the difference formulation results are smaller by a factor that decreases as the optical thickness increases. The noise in the standard formulation increases dramatically with optical depth, while the noise in the difference formulation does not. We note that these results were obtained with an implementation assuming piecewise constant material properties, which does not achieve the diffusion limit for zone sizes larger than a mean free path. Accordingly, these runs used zoning sufficiently fine to resolve a mean free path. An implementation with piecewise linear properties is under development.

The particle counts in these calculations were set so that the Monte Carlo run times were the same for the two methods, and 100 runs with different random number seeds were done for each formulation. The computational advantage of the difference formulation compared to the standard formulation is shown in Figure 5, where this quantity is defined as the square of the ratio of the standard deviations of the sets of runs.

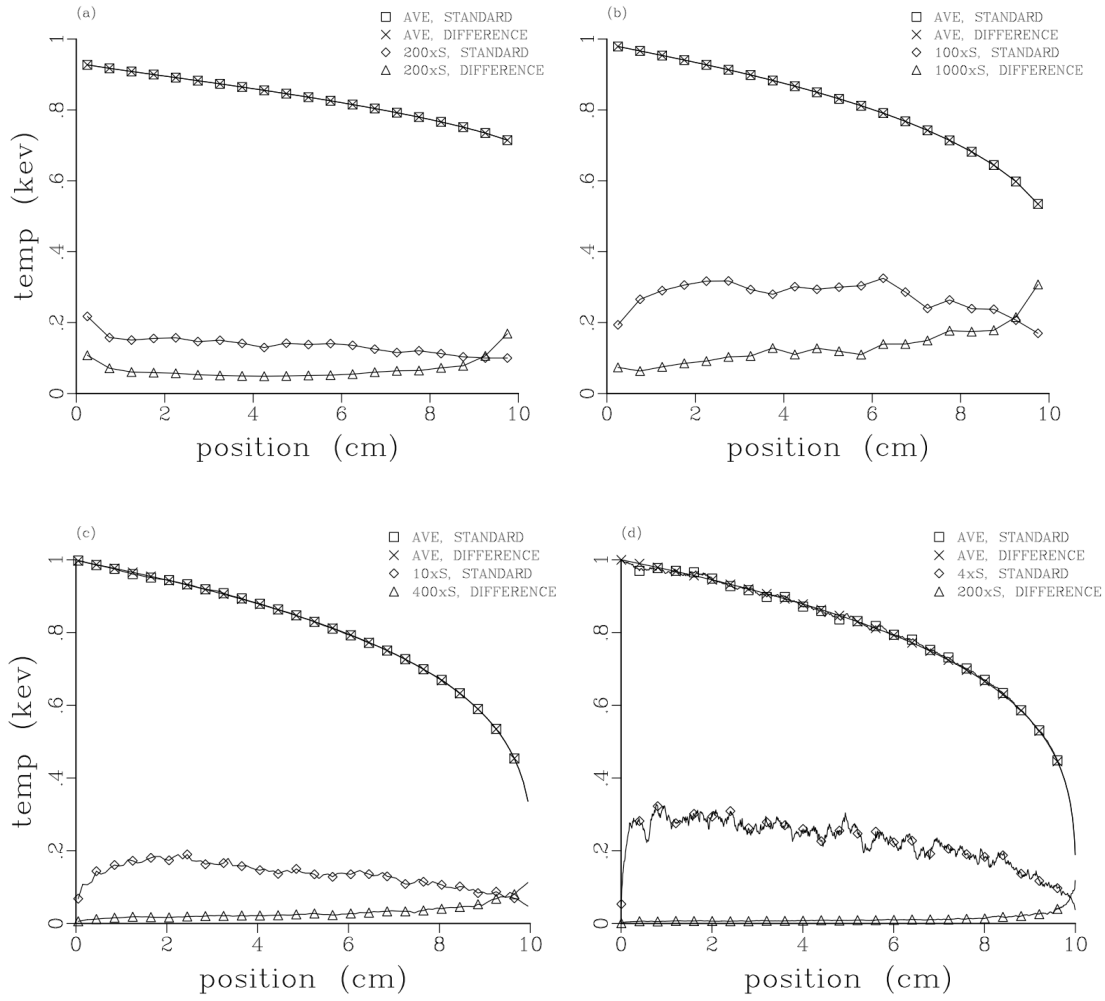

Figure 4. Temperature distribution in a slab in steady state. The total optical depth of the slab is 1 in (a), 10 in (b), 100 in (c) and 1000 in (d). The standard deviation of the difference formulation is denoted by diamonds and that of the difference formulation by triangles. Note the change in their relative scale with optical depth. Reproduced from Brooks *et al* (2005).

This implementation used SIMC for implicitness and stability. However, the difference formulation is independent of any particular discretization or solution method. Similarly, it does not mitigate deficiencies in the solution method, whether deterministic or Monte Carlo. An implementation using IMC rather than SIMC also shows improved performance / decreased noise, but retains the timestep limitations of IMC.

The difference formulation enjoys a significant performance advantage over standard Monte Carlo in opaque regions. Experiences to date also show comparable performance to standard Monte Carlo in transparent regions, leading to the possibility of reducing statistical noise by simply using the difference formulation over the entire problem domain.

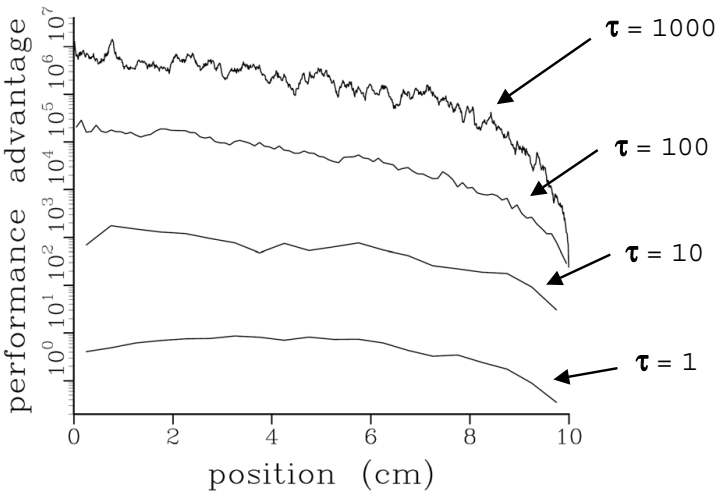

Figure 5. The relative computational advantage of the difference formulation compared to the of the standard formulation, plotted as a function of position for various optical depths of the slab. Reproduced from Brooks *et al* (2005).

Acknowledgements

This work was performed under the auspices of the U. S. Department of Energy by University of California Lawrence Livermore National Laboratory under contract No. W-7405-ENG-48.

References

Fleck, J. A., Jr., in *Computational Methods in the Physical Sciences*, Alder, B. and Fernbach, S. (McGraw-Hill, New York, 1963), Vol 1, 43-65.

Fleck, J. A., Jr. and Cummings, J. D., "An implicit Monte Carlo scheme for calculating time and frequency dependent nonlinear radiation transport," *J. Comput Phys.* **8**, 313–342 (1971).

Graziani, F., and LeBlanc, J. "The crooked pipe test problem," UCRL-MI-143393 (2000)

Gentile, N. A., "Implicit Monte Carlo diffusion - an acceleration method for Monte Carlo time-dependent radiative transfer simulations," *J. Comput Phys.* **172**, 543–571 (2001).

Nowak, P. and Nemanic, M. "Proceedings of the ANS Conference on Mathematics and Computation, Reactor Physics, and Environmental Analysis in Nuclear Applications," Madrid, Spain, 379-390 (1999)

Larsen, E. W., "Diffusion theory as an asymptotic limit of transport theory for nearly critical systems with small mean free paths," *Ann. Nucl Ener.* **7**, 249-256 (1980).

Fleck, J. A., Jr., and Canfield, E. H., "A random walk procedure for improving the computational efficiency of the Implicit Monte Carlo method for nonlinear radiation transport", *J. Comput. Phys* **54**, 508-523 (1984)